

# DIRECT OXIDATION OF METHANE TO METHANOL OVER Cu-ZEOLITES AT MILD CONDITIONS

**Mauro Álvarez, Pablo Marín, Salvador Ordóñez\***

Department of Chemical and Environmental Engineering, University of Oviedo,  
Faculty of chemistry, Julián Clavería 8, 33006 Oviedo, SPAIN.

(\*Phone: 34-985 103437. E-mail: [sordonez@uniovi.es](mailto:sordonez@uniovi.es))

## Abstract

The partial oxidation of methane to methanol over a Cu-Na-MOR catalyst is studied in this work. The reaction, performed in a fixed-bed reactor, is accomplished according to a three steps cycling process: adsorption of methane, desorption of methanol promoted by water and regeneration of the catalyst. The operating conditions of the different steps of the process have been optimized to maximize methanol yield. The regeneration using air, instead of pure oxygen, has been found to increase methanol yield in the following cycle. Optimum desorption is carried out using water concentration of 5.2 mol% and  $3.04 \text{ Nm}^3 \text{ h}^{-1} \text{ kg}^{-1}_{\text{cat}}$ . At the optimal conditions, the yield of methanol raised to  $754 \mu\text{mol/g Cu}$ , corresponding to 52% of adsorbed methane being transformed into methanol.

**Keywords:** Methane upgrade; mordenite; methanol; cyclic reactors; partial oxidation.

## CRedit author statement

**Mauro Álvarez:** Investigation, Writing- Original draft preparation

**Pablo Marín:** Methodology, Supervision, Validation

**Salvador Ordóñez:** Conceptualization, Supervision, Writing- Reviewing and Editing

## 1. Introduction

Methanol is widely used in industry as solvent, fuel additive or feedstock for the production of other chemicals [1-4]. The current technology for methanol manufacturing is based on the production of syngas from methane raw material via steam reforming. This process is energy and capital intensive and, for this reason, the search of a process for the direct conversion of methane to methanol is of great interest [5-9]. However, the C-H bond on methane molecule is the strongest among all the hydrocarbons [10, 11], requiring harsh reaction conditions (e.g. temperature) to activate it. At high reaction temperature, overoxidation of methanol to carbon oxides may take place even in presence of catalyst, making this process very challenging [12-17].

In the last years, the research in this field has been focused on the development of a catalyst able of activating methane at low temperature and preventing further oxidation to carbon oxides. Different types of catalysts have been proposed, which are classified as homogeneous (e.g. [18-20]) and heterogeneous (e.g. [20-22]). Heterogeneous catalysts are a better option from the point of view of a future industrial application. Indeed, the product recovery is easier, their cost is lower and the operating conditions are mild (most homogeneous catalysts are based on the use of strong acid conditions).

The direct oxidation of methane to methanol at mild and aerobic conditions is a reaction that actually occurs in microorganisms catalyzed by methane mono-oxygenase (MMO) enzymes. There are two known types of MMO enzymes: soluble (sMMO) and particulate (pMMO). These enzymes contain diiron and dicopper active centers responsible of the activation of methane molecules [23, 24]. The development of a heterogeneous catalyst for this reaction has been focused on mimicking the structure of the active site found in these enzymes. On the other side, zeolites are materials with highly ordered internal structure, formed by parallel channels of regular size. These materials are good candidates to host metallic centers similar to those of pMMO [13, 25].

Many zeolite topologies have been studied [26-29], but copper exchanged mordenites (Cu-MOR) catalysts have emerged as the most interesting ones. Their high yield towards methanol and large pores facilitate the desorption of the products from the active centers [16, 30]. Nowadays, there is still no consensus about the active site configuration. Many works indicate that bis( $\mu$ -oxo)dicopper active sites are the only ones responsible of the catalytic behavior. However, other works suggest that mono( $\mu$ -oxo)dicopper and trinuclear copper-oxo clusters can also be active [31, 32].

The oxygen of the active site reacts with methane, leading to intermediate adsorbed methoxy species. At low reaction temperature, these species are strongly adsorbed on the active site, preventing other methane molecules adsorption and stopping the reaction. If temperature is increased to promote desorption and methanol formation, the undesired overoxidation to carbon oxides takes place [33].

To recover methanol, liquid [24] or vapor [13] water is introduced in the reactor. The role of water on this step is still under discussion, but many authors suggest it can be twofold. On one hand, water can displace methanol from the active centers by competitive adsorption and, on the other hand, it stabilizes the reaction intermediates [9, 24].

These two steps, adsorption and desorption, are performed at 200°C or below to minimize undesired overoxidation reactions [6, 13]. In contact with water, the copper clusters are hydrolyzed and therefore deactivated [34]. Thus, the material needs to be dehydrated and re-oxidized at high temperature, before reuse. A cheap and available oxidant, such as oxygen or air, would be preferred in view of a future industrial process [23, 35].

Summarizing, the overall reaction corresponds to a cyclic process formed by three steps: (1) methane adsorption, (2) methanol desorption and (3) oxidative regeneration of the catalyst [2, 14]. This process has been studied for the upgrading of methane emissions on remote oil exploitations [9], which otherwise are exhausted or flared depending on local regulations [36, 37]. However this direct conversion process brings the possibility of harnessing other emissions with lower methane concentration, such as those related to coal mining or waste management [38-40].

In the present work, the reactivity of Cu-MOR catalyst for the direct oxidation of methane to methanol has been explored. The catalyst has been prepared via aqueous ion-exchange of a commercial Na-MOR. The reaction studies have been performed in a stainless steel fixed-bed reactor loaded with 3 g of catalyst with a particle size in the range 0.355-1 mm that forms a catalytic bed of 110 mm. This is a step further in reactor size compared to previous works from the literature about this reaction. Thus, in these works, the reactor is considerably smaller with much lower amounts of catalyst (up to 0.7 g [16, 41]), smaller particles sizes (up to 0.500 mm [9, 42]) and bed lengths (up to 1.4 cm [14]). The present work is aimed at demonstrating that methanol can be obtained from methane in quantitative amounts according to a step-wise cycling process. For this reason, the use of a larger reactor is of great importance, as a first step towards the scale-up of the process. The operating conditions of the different steps have also been optimized in order to maximize the yield of methanol.

## **2. Materials and methods**

### **2.1. Catalyst preparation**

Mordenite zeolite (Na-MOR, Si/Al = 6.5, CBV10A), supplied from Zeolyst International, was used to prepare the catalyst by ion exchange with a copper solution. The zeolite (10 g) was mixed with 0.01 M copper (II) acetate solution (780 mL). The mixture was stirred for 24 hours at room temperature and filtered [24, 43]. The precipitation of Cu(OH)<sub>2</sub> was avoided by maintaining the pH at 5.7 [23, 42]. The exchange procedure was repeated three times to increase copper loading. After the last exchange, the filtrate was rinsed with distilled water and dried at 110°C overnight. The dried catalyst was pelletized and sieved to the desired particle size (0.355-1 mm). Finally, the catalyst is activated in an oxygen gas flow using a temperature at 450°C (ramp of 1°C/min, hold 4 h).

### **2.2. Catalyst characterization**

Copper loading of the catalyst was determined by dissolving the sample in aqua regia and analyzing the resulting liquid by ICP-MS. The textural properties (surface area and

pore volume) were determined by nitrogen adsorption using a Micromeritics ASAP 2020 Plus (before the analysis, the samples were degassed under vacuum at 150 °C for 10 h).

X-ray powder diffraction (XRD) analysis were performed in a Bruker D8 Discover to obtain information about the crystallographic structure of the zeolite before and after the ion exchange procedure. Transmission electron microscopy (TEM) measurements were carried out in both bright and dark field contrasts using a MET JEOL-JEM 2100F microscope to study the dispersion of copper in the zeolite structure.

### **2.3. Experimental device**

The reaction was studied in a tubular stainless steel fixed-bed reactor (internal diameter 6.8 mm). The reactor tube was loaded with 3 g of catalyst, maintained in a fixed position using a porous plug. The catalytic bed had a length of 110 mm. The reactor configuration fulfills the requirement to ensure plug flow pattern through the catalytic bed [44]: ratio of reactor inner diameter to catalyst particle size at least 10 (in this case, it is exactly 10) and ratio of bed length to catalyst particle size higher than 50 (in this case, it is 162). The existence of plug flow inside the reactor is essential to prevent a bad distribution of the reactants and channeling.

The tube was filled with glass spheres (1 mm) upstream the catalytic bed, in order to pre-heat the feed. The tube was surrounded by an electrical oven, the temperature is controlled using a thermocouple placed inside the reactor tube very close to the catalytic bed.

The flowsheet of the experimental device is depicted in Figure 1. The gases (methane, nitrogen, oxygen and air) are supplied from cylinders (Air Liquide) and their flowrate is set using mass flow controllers (Bronkhost). The reactor feed is prepared by mixing the corresponding gases in adequate proportions. No appreciable pressure drop was observed in the reactor operating at atmospheric pressure.

A syringe pump is used to feed the liquid water and mix it with the hot nitrogen stream, causing its vaporization. To prevent the occurrence of water concentration

pulses during the vaporization, a mixing tank of 1 L was placed downstream the water injection point. This tank and all the pipes from the injection point to the reactor inlet are covered with heating tape, maintained at 150°C to prevent condensation.

The composition of the reactor effluent can be analyzed on-line or off-line. The on-line analysis is carried out continuously, using a mass spectrometer (MS) OmniStar GSD 301. However, the measurements of this kind of equipment can be easily interfered by the presence of water (in great amount during methanol desorption).

The off-line analysis is based on the use of a cold trap that condenses methanol and water of the reactor effluent during the desorption step. The cold trap consists of an U-tube made of borosilicate glass and placed inside an isopropanol/liquid nitrogen bath (temperature -50°C). The condensate is accumulated in the U-tube during the desorption step. Then, the liquid sample is collected and the species analyzed in a gas chromatograph (GC) Shimadzu GC-2010 equipped with a CP-Sil 8CB column and a flame ionization detector (FID). Ethyl acetate is used as internal standard. The estimated relative standard deviation for this analytical method is 7.4%. The non-condensable gases leave the cold trap and are analyzed in the mass spectrometer. To prevent condensation of water or any product, the reactor the outlet pipes were also covered with heating tape maintained at 150°C.

#### **2.4. Reaction tests**

The reaction of direct oxidation of methane to methanol was carried out according to a three-step cyclic process: adsorption, desorption and regeneration [24]. Figure 2 shows a sketch of the step and their operating conditions, as discussed below. In the adsorption step, a methane stream of 120 mL n.t.p./min ( $WHSV = 2.29 \text{ Nm}^3 \text{ h}^{-1} \text{ kg}_{\text{cat}}^{-1}$ ) is fed at 200°C and 1 atm for 20 min. Then, methanol desorption is promoted by feeding a flow of water in nitrogen gas at 150°C and 1 atm for 4 h. The flow rates of water and nitrogen were varied in the range 0.4-0.7 g/h and 150 to 220 mL n.t.p./min, respectively. Finally, the catalyst is regenerated at oxidizing conditions using a gas flow rate of 120 mL n.t.p./min ( $WHSV = 2.29 \text{ Nm}^3 \text{ h}^{-1} \text{ kg}_{\text{cat}}^{-1}$ ) of oxygen or air at 450°C and 1 atm (ramp to 450°C and hold for 4 h). This temperature was selected, because it

ensures the fully dehydration of the catalyst [35] and also maximizes the production of methanol [43]. After every step, the system was purged with nitrogen (gas flow 120 mL n.t.p./min) to eliminate remaining gases in the piping and bed voids.

Additional tests were required to quantify the amount of methane adsorbed on the catalyst in the adsorption step. Thus, after the adsorption, the reactor was heated in an air stream of 120 mL n.t.p./min ( $WHSV = 2.29 \text{ Nm}^3 \text{ h}^{-1} \text{ kg}_{\text{cat}}^{-1}$ ) at a rate of  $10^\circ\text{C}/\text{min}$  up to  $450^\circ\text{C}$ . This caused the total oxidation of the adsorbed methane to  $\text{CO}_2$ , which is analyzed on-line by MS (signal of  $m/z = 44$ ) [16, 24]. The  $\text{CO}_2$  signal of the MS can be used to quantify the amount of methane previously adsorbed on the catalyst using a calibration. The decomposition of a sodium bicarbonate sample of known weight was used to calibrate the MS [9]).

### **3. Results and discussion**

#### **3.1. Catalyst characterization results**

The preparation of the catalyst was done by ion exchange on commercial zeolites. The procedure was repeated three times to increase the copper loading up to 4.5 wt% (ICP-MS) in the fresh catalyst. This value is very similar to those reported in the bibliography for similar catalysts (e.g. 4.3 wt% [24]). The copper content of the catalyst after being used in 19 reaction cycles was analyzed again and a loading of 4.5 wt% was obtained. This indicates that copper is not lost during the reaction.

According to the results presented in Table 1, the BET surface area and micropore volume of the zeolite slightly decrease when the copper is introduced in its structure. This can be explained by the blockage of some pores with copper oxide clusters of large size [23, 42]. The properties of the catalyst after 19 reaction cycles are similar to those of the fresh catalyst, which means that its structure does not change during the reaction process.

XRD measurements before and after the ion-exchange procedure are displayed in Figure 3. After the addition of copper, no new peaks could be detected. This suggests that the addition of copper is in the form of crystalline particles of very small size (less

than 3 nm) or non-crystalline (i.e. amorphous) phase [16]. Nonetheless, a decrease in peak intensity is observed after the addition of copper, which is attributed to a decrease in crystallinity. Scherrer equation ( $\tau = k \cdot \lambda / \beta \cdot \cos\theta$ ) was used to estimate this decrease: 20% lower compared to the fresh zeolite support.

Considering that the solid only have two phases, copper oxide the most dense and dark, and the zeolite less dense, it is possible to qualitatively estimate dispersions by TEM. The larger copper oxides crystallites (Figure 4A) are on the surface of the catalyst, while the smaller ones seem to be inside the zeolite pores (Figure 4B). The larger clusters are attributed to amorphous copper oxide, since no new peaks were found in the XRD spectra. The smaller clusters have a size in the range 1.37-2.81 nm. The activation of methane is attributed to these small clusters, as is indicated in the bibliography [7].

### **3.2. Preliminary reaction studies**

The first reaction experiments were aimed to demonstrate that the Cu-MOR catalyst is able to catalyze the partial oxidation of methane to methanol. The general experimental reaction procedure was detailed in section 2.4. As explained, the reaction is accomplished in three steps: adsorption, desorption and regeneration.

In the preliminary tests, the desorption step was carried out using a N<sub>2</sub> flow rate of 220 mL n.t.p./min (WHSV = 4.42 Nm<sup>3</sup> h<sup>-1</sup> kg<sup>-1</sup><sub>cat</sub>) and a water concentration of 4.5 mol%. During the 4 h of the desorption step, a total amount of 2 g of water were introduced in the reactor, from which 74% were recovered as sample in the cold trap. This sample was analyzed by GC and methanol concentration was 30 mmol/L. Considering the sample mass (1.48 g), the amount of catalyst in the reactor (3.12 g) and its copper loading (4.5 %), the yield of methanol was determined: 330 μmol/g Cu. The regeneration was done with an oxygen gas flow and using a temperature ramp of 1°C/min up to 450°C (hold 4 h).



The reaction cycle was repeated three times for the same catalyst batch and the operating conditions indicated above. The average yield of methanol was a value of 327  $\mu\text{mol/g Cu}$  with a relative standard deviation of 2.5%. These results suggest that the regeneration step is able to restore the catalytic activity and, hence, prove that the catalyst can be reused in the cycling process.

The performance of another batch of catalyst, prepared according to the same methodology, was also studied. In this case, the yield of methanol at the abovementioned conditions was 307  $\mu\text{mol/g Cu}$ , which is only 6% lower than that of the first batch. Consequently, it can be confirmed the good reproducibility of the different stages involved in the experimental procedure (i.e. catalyst preparation, reaction testing and sample analysis).

### **3.3. Optimization of operating conditions**

Once the catalyst has demonstrated its activity towards methanol in the partial oxidation reaction of methane, the studies have been focused on optimizing the operating conditions. The aim of this section is to determine the influence of the experimental conditions of the different steps of the process, in order to maximize the yield of methanol.

#### **3.3.1. Optimization of the regeneration step**

The regeneration step of the preliminary reaction tests was carried out using an oxygen gas flow and a temperature ramp of 1°C/min. Such a low ramp increased considerably the time required for the regeneration. In order to reduce the regeneration time, faster temperature ramps have been considered. The final regeneration temperature and the hold time remained identical (450°C and 4 h, respectively).

Figure 5 shows the impact of temperature ramps in the range 1 to 5°C/min on the yield of methanol obtained in the following reaction cycle. Thereby, if the regeneration were not adequate in one cycle, methanol yield would be reduced in the following one. An increase of the ramp to 2°C/min has no influence on methanol yield,

311  $\mu\text{mol/g Cu}$ , only 5% lower than that obtained at  $1^\circ\text{C}/\text{min}$  (i.e. close to the reproducibility confidence interval, as discussed in the previous section). However, the increase to a ramp of  $5^\circ\text{C}/\text{min}$  has a marked negative consequence on methanol yield, reducing it to 171  $\mu\text{mol/g Cu}$ . This can be explained by the reduction of the total regeneration time, which is reduced to 5.5 h, half of the time than with a ramp of  $1^\circ\text{C}/\text{min}$ , causing an incomplete regeneration of the catalytic activity.

Some works [41] have reported that methanol yield decreases when oxygen pressure used in the regeneration step is increased above 1 bar. For this reason, a study of the impact of oxygen partial pressure below 1 bar has been proposed in the present work. In particular, the regeneration step has been done using synthetic air (20% oxygen in nitrogen) instead of pure oxygen. The results, shown in Figure 5, indicate that oxygen partial pressure has a marked influence on methanol yield, an increase of 58% with 504  $\mu\text{mol/g Cu}$  (with a ramp of  $1^\circ\text{C}/\text{min}$ ) being observed when using air as regenerant. A similar increase is also obtained for the ramp of  $2^\circ\text{C}/\text{min}$ , whereas at higher heating rates the methanol yield markedly decreases.

This is an important finding, since air is a cheaper oxidant. Consequently, the following operating conditions are found to be optimal for the regeneration step: air gas flow and a temperature ramp of  $2^\circ\text{C}/\text{min}$  up to  $450^\circ\text{C}$ . In the next studies of the present work, these conditions will be used.

### 3.3.2. Optimization of the desorption step

The desorption step is the part of the process where methanol is recovered from the catalyst. This is accomplished by gaseous water in a nitrogen flow. At low temperature ( $150^\circ\text{C}$ ), water causes the desired methanol desorption. This section is focused on the study of the influence of water concentration and gas flow during the desorption step.

The preliminary reactions were carried out using a  $\text{N}_2$  flow of 220 mL n.t.p./min and a water concentration of 4.5 mol%. Figure 6 summarizes the experimental results, corresponding to water concentration in the range 3.2-7.7 mol% and  $\text{N}_2$  flow rate 150-220 mL n.t.p./min. At 220 mL n.t.p./min, methanol yield increased to 609  $\mu\text{mol/g Cu}$ , when water concentration increased from 4.5 to 6.2 mol%. This behavior can be

related to the shift of the methanol adsorption equilibrium caused by the increase on the water concentration.

However, the best improvement in methanol yield was observed when the N<sub>2</sub> flow rate was reduced to 190 or even 150 mL n.t.p./min, both with similar results in the range 700-750 μmol/g Cu. At 150 and 190 mL n.t.p./min, the influence of water concentration is slightly different to that observed at 220 mL n.t.p./min. Thus, on increasing water concentration, methanol yield increases, has a maximum at 5.2 mol% and, then, decreases slowly. At 220 mL n.t.p./min, the maximum was not observed, because of falling outside of the experimental region.

Considering these results, the optimal conditions for the desorption step are: N<sub>2</sub> flow rate of 150 mL n.t.p./min (WHSV = 3.04 Nm<sup>3</sup> h<sup>-1</sup> kg<sub>cat</sub><sup>-1</sup>) and water concentration 5.2 mol%; at these conditions, 754 μmol/g Cu were produced.

### **3.4. Quantification of the reactor performance at the optimal operating conditions**

~~The optimal conditions for the operation of the reactor were determined in the previous section. Adsorption with pure methane (120 mL n.t.p./min) at 200°C for 20 min. Desorption with 5.2 mol% water in nitrogen gas (total gas flow 160 mL n.t.p./min) at 150°C for 4 h. Catalyst regeneration in synthetic air (120 mL n.t.p./min, 20% O<sub>2</sub> in nitrogen) at 450°C (1°C/min ramp) for 4 h.~~

The optimal conditions for the operation of the reactor, determined in the previous section, are summarized in Table 2.

In this section, the performance of the individual reaction steps has been studied at the optimum conditions. First, a test has been proposed to quantify the amount of methane adsorbed on the catalyst during the adsorption step. This test consists of a convectional adsorption step with methane at 200°C, followed by a temperature programmed desorption (rate of 10°C/min) in an air gas flow (no water is added). Since methane is adsorbed strongly, an increase of temperature is required, which causes its oxidation to carbon dioxide. This gas is analyzed on-line using the MS (signal m/z = 44), as shown in the curves represented on Figure 7. The presence of two CO<sub>2</sub>

peaks, at 210 and 270°C suggests that there are two different kind of active centers on the catalyst. The CO<sub>2</sub> peak obtained at low temperature, which is the larger one, corresponds to mildly adsorbed methane; note that the adsorption step was carried out at 200°C and this peak is produced at 210°C. Using the calibration of the CO<sub>2</sub> signal of the MS, an estimation of the amount of adsorbed methane can be obtained: 1482 μmol/g Cu, from which 911 μmol/g Cu corresponds to the first peak and 571 μmol/g Cu to the second. The yield of methanol obtained in the desorption step was 754 μmol/g Cu, which means that 52% of the adsorbed methane is able to react to methanol.

The test (adsorption and temperature-programed desorption) was repeated twice to check the reproducibility. As depicted in Figure 7, both MS signals overlap completely. The reactor effluent was also analyzed using the MS during the regeneration step. As shown in Figure 8, a small CO<sub>2</sub> peak (signal m/z = 44) was produced at 200°C. This means that a small part of the adsorbed methane cannot be upgraded to methanol during the desorption step. On increasing temperature as part of the regeneration step, this methane is oxidized to CO<sub>2</sub> and desorbed. The amount of CO<sub>2</sub> generated in the regeneration step is 106 μmol CO<sub>2</sub>/g Cu, which is only 7% of the amount of adsorbed methane. Differently to the temperature programmed test previously discussed, where there were two CO<sub>2</sub> peaks, only the first peak is produced during the regeneration step. Thus, part of the mildly adsorbed methane (attributed to the 210°C CO<sub>2</sub> peak of the temperature programmed test) can be in active centers which are not associated to methanol formation and, for this reason, this methane remained the same after the (water) desorption step at 150°C. Figure 8 also depicts the MS signal of m/z = 18 attributed to water. During the regeneration of the catalyst, all the water should be desorbed and the copper active phase re-oxidized. The maximum of the water peak is produced at 135°C, but water is still present in the reactor effluent up to around 300°C. The maximum regeneration temperature (450°C) guarantees the fully dehydration of the catalyst.

Considering the results previously reported a yield to methanol of 52% was obtained at these optimal conditions, while 7% of the methane adsorbed was oxidized to CO<sub>2</sub> during the activation step (Figure 9). The rest of the methane adsorbed is considered

to be bonded weaker to the active centers, being fully oxidized to CO<sub>2</sub> during the desorption step.

### **3.5. Catalyst stability**

In the preliminary reactions performed in section 3.2, it was demonstrated that the regeneration step restored the catalytic activity of the Cu-MOR catalyst, after three consecutive reaction cycles. However, it would be interesting to analyze the medium to long term stability of the catalytic.

The yield of methanol at the optimum operating conditions was 754 μmol/g Cu. After 18 reactions, the yield decreased to 725 μmol/g Cu. Thus, the yield decreased 3.9%, which is within the estimated reproducibility of the reaction (relative standard deviation of 2.5%, as discussed section 3.2). In other words, the loss of catalytic activity can be considered negligible.

## **4. Conclusions**

The performance of a Cu-MOR catalyst used for the direct conversion of methane to methanol has been investigated in a fixed-bed reactor. The reaction is accomplished according to a cyclic process made of three steps: adsorption, desorption and regeneration. It has been demonstrated that methanol can be synthesized by this method at mild conditions (200°C and 1 atm) and the catalytic activity is preserved after several reaction cycles.

The operating conditions of the different steps have been optimized in order to maximize the yield of methanol. The regeneration step is carried out at high temperature, 450°C, and for 4 h. On one hand, it has been evidenced that the use of temperature ramps higher than 5°C/min to reach the final regeneration temperature have a negative impact on the yield of methanol. On the other hand, the use of air during the regeneration, instead of oxygen, produces an increase of the yield of methanol obtained in the following cycle by 58%. The desorption step is highly

affected by the total gas flow rate and water concentration. It has been concluded that the optimal conditions are  $3.04 \text{ Nm}^3 \text{ h}^{-1} \text{ kg}_{\text{cat}}^{-1}$  and water molar fraction 5.2 mol%.

The optimization of the reaction conditions resulted in an increase of methanol yield from  $320 \mu\text{mol/g Cu}$  to  $754 \mu\text{mol/g Cu}$ . A deeper analysis of the catalyst performance at the optimum reaction conditions has revealed that 52% of the adsorbed methane is actually transformed to methanol; the rest is desorbed or oxidized to  $\text{CO}_2$  during the desorption and regeneration steps.

## Acknowledgements

This work was supported by the METHENERGY+ Project of the Research Fund for Coal and Steel (EU) [grant number 754077]. Also, authors would like to acknowledge the technical support provided by Servicios Científico-Técnicos de la Universidad de Oviedo.

## References

- [1] P. Khirsariya, R.K. Mewada, Single Step Oxidation of Methane to Methanol—Towards Better Understanding, *Procedia Eng.*, 51 (2013) 409-415. <https://doi.org/10.1016/j.proeng.2013.01.057>.
- [2] Z.-J. Zhao, A. Kulkarni, L. Vilella, J.K. Nørskov, F. Studt, Theoretical Insights into the Selective Oxidation of Methane to Methanol in Copper-Exchanged Mordenite, *ACS Catal.*, 6 (2016) 3760-3766. <https://doi.org/10.1021/acscatal.6b00440>.
- [3] Z. Zakaria, S.K. Kamarudin, Direct conversion technologies of methane to methanol: An overview, *Renew. Sust. Energ. Rev.*, 65 (2016) 250-261. <https://doi.org/10.1016/j.rser.2016.05.082>.
- [4] P.G. Lustemberg, R.M. Palomino, R.A. Gutiérrez, D.C. Grinter, M. Vorokhta, Z. Liu, P.J. Ramírez, V. Matolín, M.V. Ganduglia-Pirovano, S.D. Senanayake, J.A. Rodriguez, Direct Conversion of Methane to Methanol on Ni-Ceria Surfaces: Metal–Support Interactions and Water-Enabled Catalytic Conversion by Site Blocking, *J. Am. Chem. Soc.*, 140 (2018) 7681-7687. <https://doi.org/10.1021/jacs.8b03809>.
- [5] B. Han, Y. Yang, Y. Xu, U.J. Etim, K. Qiao, B. Xu, Z. Yan, A review of the direct oxidation of methane to methanol, *Chinese J. Catal.*, 37 (2016) 1206-1215. [https://doi.org/10.1016/S1872-2067\(15\)61097-X](https://doi.org/10.1016/S1872-2067(15)61097-X).
- [6] B. Ipek, R.F. Lobo, Catalytic conversion of methane to methanol on Cu-SSZ-13 using  $\text{N}_2\text{O}$  as oxidant, *ChemComm*, 52 (2016) 13401-13404. <https://doi.org/10.1039/C6CC07893A>.

- [7] N.V. Beznis, B.M. Weckhuysen, J.H. Bitter, Cu-ZSM-5 Zeolites for the Formation of Methanol from Methane and Oxygen: Probing the Active Sites and Spectator Species, *Catal Letters*, 138 (2010) 14-22. <https://doi.org/10.1007/s10562-010-0380-6>.
- [8] S. Al-Shihri, C.J. Richard, H. Al-Megren, D. Chadwick, Insights into the direct selective oxidation of methane to methanol over ZSM-5 zeolites in aqueous hydrogen peroxide, *Catal. Today*, (2018) In press. <https://doi.org/10.1016/j.cattod.2018.03.031>.
- [9] V.L. Sushkevich, D. Palagin, M. Ranocchiari, J.A. van Bokhoven, Selective anaerobic oxidation of methane enables direct synthesis of methanol, *Science*, 356 (2017) 523-527. <https://doi.org/10.1126/science.aam9035>.
- [10] C. Hammond, S. Conrad, I. Hermans, Oxidative methane upgrading, *ChemSusChem*, 5 (2012) 1668-1686. <https://doi.org/10.1002/cssc.201200299>.
- [11] A.A. Latimer, A. Kakekhani, A.R. Kulkarni, J.K. Nørskov, Direct Methane to Methanol: The Selectivity–Conversion Limit and Design Strategies, *ACS Catal.*, 8 (2018) 6894-6907. <https://doi.org/10.1021/acscatal.8b00220>.
- [12] K. Narsimhan, K. Iyoki, K. Dinh, Y. Roman-Leshkov, Catalytic Oxidation of Methane into Methanol over Copper-Exchanged Zeolites with Oxygen at Low Temperature, *ACS Cent. Sci.*, 2 (2016) 424-429. <https://doi.org/10.1021/acscentsci.6b00139>.
- [13] T. Sheppard, C.D. Hamill, A. Goguet, D.W. Rooney, J.M. Thompson, A low temperature, isothermal gas-phase system for conversion of methane to methanol over Cu–ZSM-5, *ChemComm*, 50 (2014) 11053-11055. <https://doi.org/10.1039/C4CC02832E>.
- [14] D.K. Pappas, E. Borfecchia, M. Dybala, I.A. Pankin, K.A. Lomachenko, A. Martini, M. Signorile, S. Teketel, B. Arstad, G. Berlier, C. Lamberti, S. Bordiga, U. Olsbye, K.P. Lillerud, S. Svelle, P. Beato, Methane to Methanol: Structure–Activity Relationships for Cu-CHA, *J. Am. Chem. Soc.*, 139 (2017) 14961-14975. <https://doi.org/10.1021/jacs.7b06472>.
- [15] J. Woertink, P. Smeets, M. Groothaert, M. Vance, B. Sels, R. Schoonheydt, E. Solomon, A [Cu<sub>2</sub>O]<sub>2</sub><sup>+</sup> core in Cu-ZSM-5, the active site in the oxidation of methane to methanol, *Proc Natl Acad Sci USA*, 106 (2009) 18908-18913. <https://doi.org/10.1073/pnas.0910461106>.
- [16] H.V. Le, S. Parishan, A. Sagaltchik, C. Göbel, C. Schlesiger, W. Malzer, A. Trunschke, R. Schomäcker, A. Thomas, Solid-State Ion-Exchanged Cu/Mordenite Catalysts for the Direct Conversion of Methane to Methanol, *ACS Catal.*, 7 (2017) 1403-1412. <https://doi.org/10.1021/acscatal.6b02372>.
- [17] K.T. Dinh, M.M. Sullivan, P. Serna, R.J. Meyer, M. Dincă, Y. Román-Leshkov, Viewpoint on the Partial Oxidation of Methane to Methanol Using Cu- and Fe-Exchanged Zeolites, *ACS Catal.*, 8 (2018) 8306-8313. <https://doi.org/10.1021/acscatal.8b01180>.
- [18] T. Zimmermann, M. Soorholtz, M. Bilke, F. Schüth, Selective Methane Oxidation Catalyzed by Platinum Salts in Oleum at Turnover Frequencies of Large-Scale Industrial Processes, *J. Am. Chem. Soc.*, 138 (2016) 12395-12400. <https://doi.org/10.1021/jacs.6b05167>.
- [19] R.A. Periana, D.J. Taube, S. Gamble, H. Taube, T. Satoh, H. Fujii, Platinum Catalysts for the High-Yield Oxidation of Methane to a Methanol Derivative, *Science*, 280 (1998) 560-564. <https://doi.org/10.1126/science.280.5363.560>.

- [20] R. Palkovits, C. von Malotki, M. Baumgarten, K. Müllen, C. Balthes, M. Antonietti, P. Kuhn, J. Weber, A. Thomas, F. Schüth, Development of Molecular and Solid Catalysts for the Direct Low-Temperature Oxidation of Methane to Methanol, *ChemSusChem*, 3 (2010) 277-282. <https://doi.org/10.1002/cssc.200900123>.
- [21] M.J. Wulfers, S. Teketel, B. Ipek, R.F. Lobo, Conversion of methane to methanol on copper-containing small-pore zeolites and zeotypes, *ChemComm*, 51 (2015) 4447-4450. <https://doi.org/10.1039/C4CC09645B>.
- [22] M.H. Mahyuddin, T. Tanaka, Y. Shiota, A. Staykov, K. Yoshizawa, Methane Partial Oxidation over  $[\text{Cu}_2(\mu\text{-O})_2]^{2+}$  and  $[\text{Cu}_3(\mu\text{-O})_3]^{2+}$  Active Species in Large-Pore Zeolites, *ACS Catal.*, 8 (2018) 1500-1509. <https://doi.org/10.1021/acscatal.7b03389>.
- [23] S. Grundner, M.A.C. Markovits, G. Li, M. Tromp, E.A. Pidko, E.J.M. Hensen, A. Jentys, M. Sanchez-Sanchez, J.A. Lercher, Single-site trinuclear copper oxygen clusters in mordenite for selective conversion of methane to methanol, *Nat. Commun.*, 6 (2015) 7546. <https://doi.org/10.1038/ncomms8546>.
- [24] E.M. Alayon, M. Nachtegaal, M. Ranocchiari, J.A. van Bokhoven, Catalytic conversion of methane to methanol over Cu–mordenite, *ChemComm*, 48 (2012) 404-406. <http://dx.doi.org/10.1039/C1CC15840F>.
- [25] S.E. Bozbag, E.M.C. Alayon, J. Pecháček, M. Nachtegaal, M. Ranocchiari, J.A. van Bokhoven, Methane to methanol over copper mordenite: yield improvement through multiple cycles and different synthesis techniques, *Catal. Sci. Technol.*, 6 (2016) 5011-5022. <https://doi.org/10.1039/C6CY00041J>.
- [26] A.R. Kulkarni, Z.-J. Zhao, S. Siahrostami, J.K. Nørskov, F. Studt, Cation-exchanged zeolites for the selective oxidation of methane to methanol, *Catal. Sci. Technol.*, 8 (2018) 114-123. <https://doi.org/10.1039/C7CY01229B>.
- [27] D.K. Pappas, E. Borfecchia, M. Dyballa, K.A. Lomachenko, A. Martini, G. Berlier, B. Arstad, C. Lamberti, S. Bordiga, U. Olsbye, S. Svelle, P. Beato, Understanding and Optimizing the Performance of Cu-FER for The Direct CH<sub>4</sub> to CH<sub>3</sub>OH Conversion, *ChemCatChem*, 11 (2019) 621-627. <https://doi.org/doi:10.1002/cctc.201801542>.
- [28] S. Erim Bozbag, P. Šot, M. Nachtegaal, M. Ranocchiari, J. Bokhoven, C. Mesters, Direct Stepwise Oxidation of Methane to Methanol over Cu-SiO<sub>2</sub>, *ACS Catal.*, 8 (2018) 5721-5731. <https://doi.org/10.1021/acscatal.8b01021>.
- [29] E.V. Kondratenko, T. Poppel, D. Seeburg, V.A. Kondratenko, N. Kalevaru, A. Martin, S. Wohlrab, Methane conversion into different hydrocarbons or oxygenates: current status and future perspectives in catalyst development and reactor operation, *Catal. Sci. Technol.*, 7 (2017) 366-381. <https://doi.org/10.1039/C6CY01879C>.
- [30] P. Vanelderen, B. E R Snyder, M.-L. Tsai, R. Hadt, J. Vancauwenbergh, O. Coussens, R. Schoonheydt, B. Sels, E. I Solomon, Spectroscopic Definition of the Copper Active Sites in Mordenite: Selective Methane Oxidation, *J. Am. Chem. Soc.*, 137 (2015) 6383-6392. <https://doi.org/10.1021/jacs.5b02817>.



- [31] M. Ravi, M. Ranocchiari, J.A. van Bokhoven, The Direct Catalytic Oxidation of Methane to Methanol—A Critical Assessment, *Angew. Chem. Int. Ed.*, 56 (2017) 16464-16483. <https://doi.org/doi:10.1002/anie.201702550>.
- [32] V.L. Sushkevich, D. Palagin, J.A. van Bokhoven, The Effect of the Active-Site Structure on the Activity of Copper Mordenite in the Aerobic and Anaerobic Conversion of Methane into Methanol, *Angew. Chem. Int. Ed.*, 57 (2018) 8906-8910. <https://doi.org/doi:10.1002/anie.201802922>.
- [33] W. Taifan, J. Baltrusaitis, CH<sub>4</sub> conversion to value added products: Potential, limitations and extensions of a single step heterogeneous catalysis, *Appl. Catal., B*, 198 (2016) 525-547. <https://doi.org/10.1016/j.apcatb.2016.05.081>.
- [34] H.A. Doan, Z. Li, O.K. Farha, J.T. Hupp, R.Q. Snurr, Theoretical insights into direct methane to methanol conversion over supported dicopper oxo nanoclusters, *Catal Today*, 312 (2018) 2-9. <https://doi.org/10.1016/j.cattod.2018.03.063>.
- [35] A.J. Knorpp, M.A. Newton, A.B. Pinar, J.A. van Bokhoven, Conversion of Methane to Methanol on Copper Mordenite: Redox Mechanism of Isothermal and High-Temperature-Activation Procedures, *Ind. Eng. Chem. Res.*, 57 (2018) 12036-12039. <https://doi.org/10.1021/acs.iecr.8b01183>.
- [36] A. Jenelle Knorpp, A. Belen Pinar, M. Newton, V. L. Sushkevich, J. A. van Bokhoven, Copper-Exchanged Omega (MAZ) Zeolite: Copper-concentration Dependent Active Sites and its Unprecedented Methane to Methanol Conversion, *ChemCatChem*, 10 (2018) 5593-5596. <https://doi.org/10.1002/cctc.201801809>.
- [37] L. Høglund-Isaksson, W. Winiwarter, P. Purohit, P. Rafaj, W. Schopp, Z. Klimont, EU low carbon roadmap 2050: Potentials and costs for mitigation of non-CO<sub>2</sub> greenhouse gas emissions, *Energy Strateg. Rev.*, 1 (2012) 97-108. <https://doi.org/10.1016/j.esr.2012.05.004>.
- [38] I. Karakurt, G. Aydin, K. Aydiner, Sources and mitigation of methane emissions by sectors: A critical review, *Renew. Energ.*, 39 (2012) 40-48. <https://doi.org/10.1016/j.renene.2011.09.006>.
- [39] A. Setiawan, E.M. Kennedy, M. Stockenhuber, Development of Combustion Technology for Methane Emitted from Coal-Mine Ventilation Air Systems, *Energy Technol.*, 5 (2017) 521-538. <https://doi.org/10.1002/ente.201600490>.
- [40] S. Su, A. Beath, H. Guo, C. Mallett, An assessment of mine methane mitigation and utilisation technologies, *Prog. Energy Combust. Sci.*, 31 (2005) 123-170. <https://doi.org/10.1016/j.pecs.2004.11.001>.
- [41] P. Tomkins, A. Mansouri, S. E. Bozbag, F. Krumeich, M. Bum Park, E. Mae C Alayon, M. Ranocchiari, J. Bokhoven, Isothermal Cyclic Conversion of Methane into Methanol over Copper-Exchanged Zeolite at Low Temperature, *Angew. Chem. Int. Ed.*, 55 (2016) 5467-5471. <https://doi.org/10.1002/anie.201511065>.
- [42] S. Grundner, W. Luo, M. Sanchez-Sanchez, J.A. Lercher, Synthesis of single-site copper catalysts for methane partial oxidation, *ChemComm*, 52 (2016) 2553-2556. <https://doi.org/10.1039/C5CC08371K>.

[43] Y. Kim, T.Y. Kim, H. Lee, J. Yi, Distinct activation of Cu-MOR for direct oxidation of methane to methanol, *ChemComm*, 53 (2017) 4116-4119. <https://doi.org/10.1039/C7CC00467B>.

[44] C. Perego, S. Peratello, Experimental methods in catalytic kinetics, *Catal Today*, 52 (1999) 133-145. [https://doi.org/10.1016/S0920-5861\(99\)00071-1](https://doi.org/10.1016/S0920-5861(99)00071-1).

## Figure captions

Figure 1. Flowsheet of the experimental device used in this work.

Figure 2. Temperature conditions and stream composition for three-step cycling process studied.

Figure 3. XRD spectra of Na-MOR (brown) and Cu-Na-MOR (blue). Crystallinity of the Cu-Na-MOR is 20% lower than the fresh zeolite and no new peaks related to crystalline copper oxide clusters are observed.

Figure 4. Transmission Electron Microscopy (TEM) images obtained for copper exchanged mordenite.

Figure 5. Effect of regeneration gas composition and temperature ramp on methanol yield. Symbols: activation with pure oxygen (●) and activation with synthetic air (◆).

Figure 6. Effect of desorption gas composition and flow rate on methanol yield. Symbols: 150 mL N<sub>2</sub> n.t.p./min (■), 190 mL N<sub>2</sub> n.t.p./min (▲) and 220 mL N<sub>2</sub> n.t.p./min (◆).

Figure 7. Mass spectrometer CO<sub>2</sub> signal ( $m/z = 44$ ) produced when heating the reactor (10°C/min) in air, after the adsorption step. Black and red curves represent consecutive experiments.

Figure 8. Mass spectrometer signals obtained during the regeneration of the catalyst for CO<sub>2</sub> ( $m/z = 44$ , black curve) and H<sub>2</sub>O ( $m/z = 18$ , blue curve).

Figure 9. Percentage of the CH<sub>4</sub> adsorbed on the catalyst (1482 μmol/g Cu) that is transformed into methanol (Blue: 754 μmol/g Cu), fully oxidized during desorption (Yellow: 608 μmol/g Cu) and eliminated during the activation of the catalyst (Green: 106 μmol/g Cu).

Figure 1

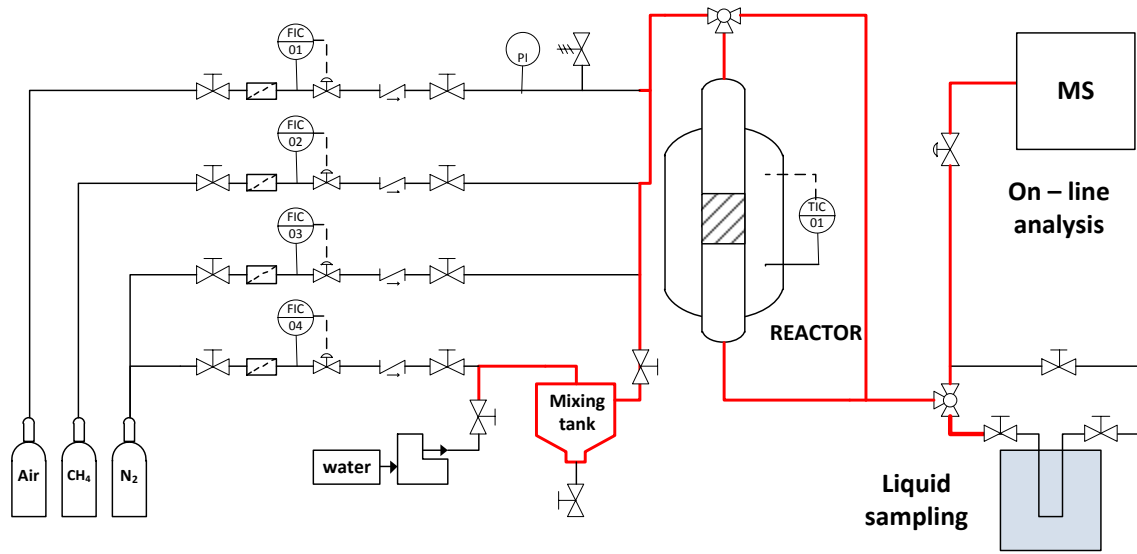


Figure 2

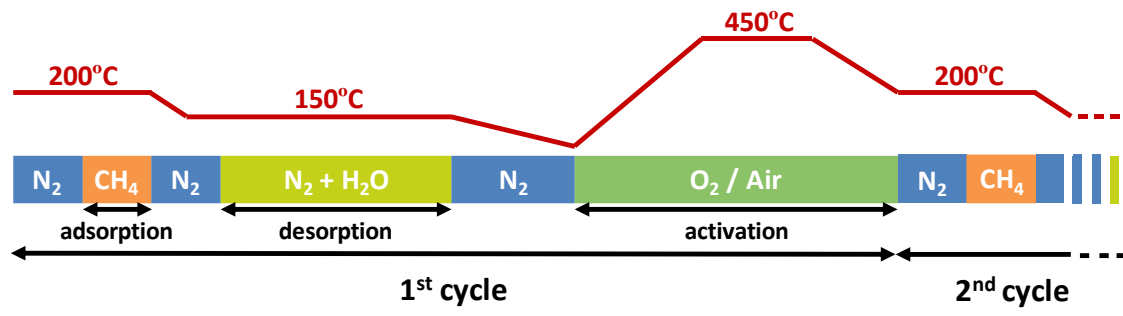


Figure 3

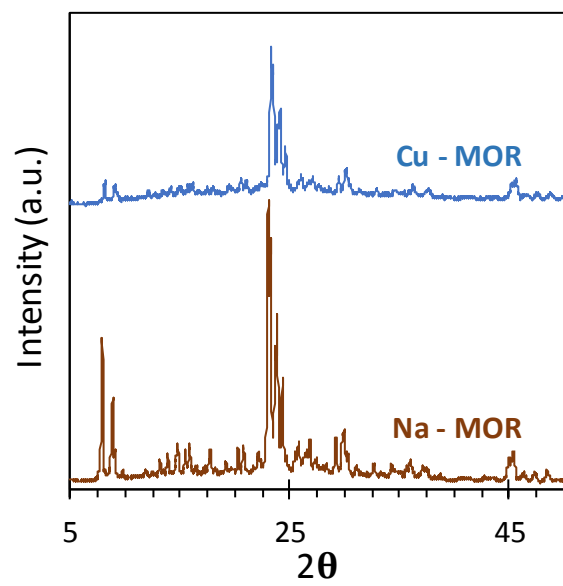


Figure 4

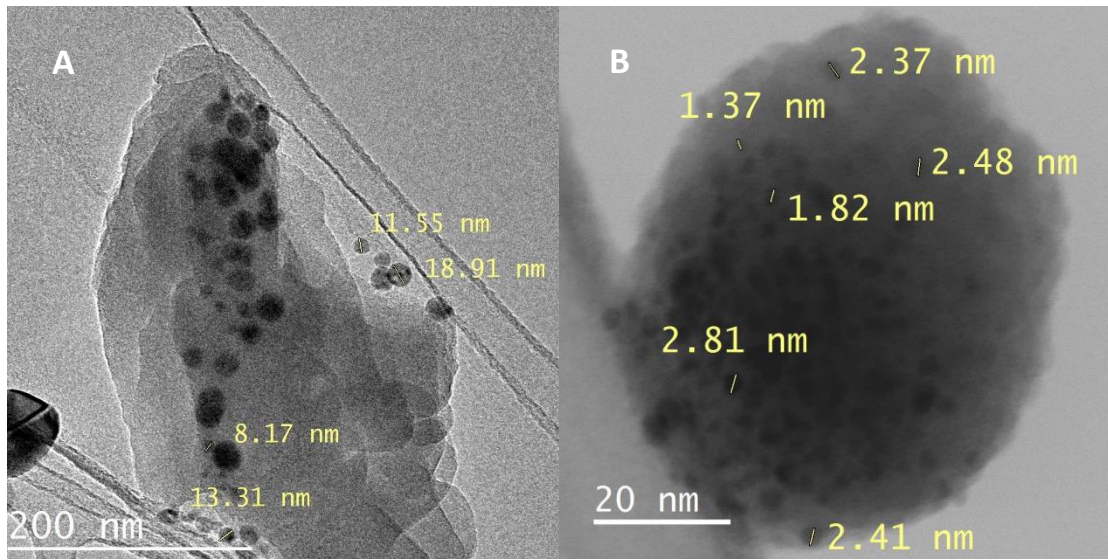


Figure 5

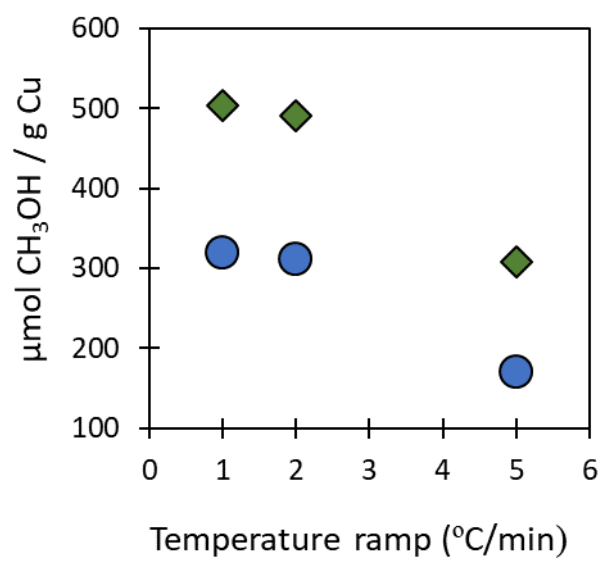




Figure 6

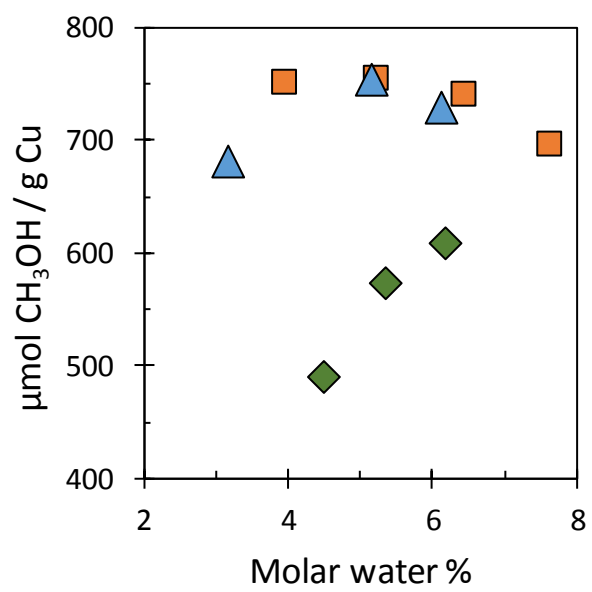


Figure 7

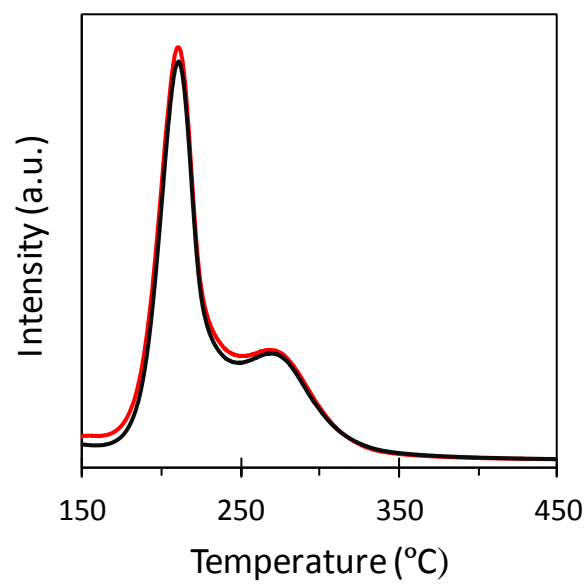


Figure 8

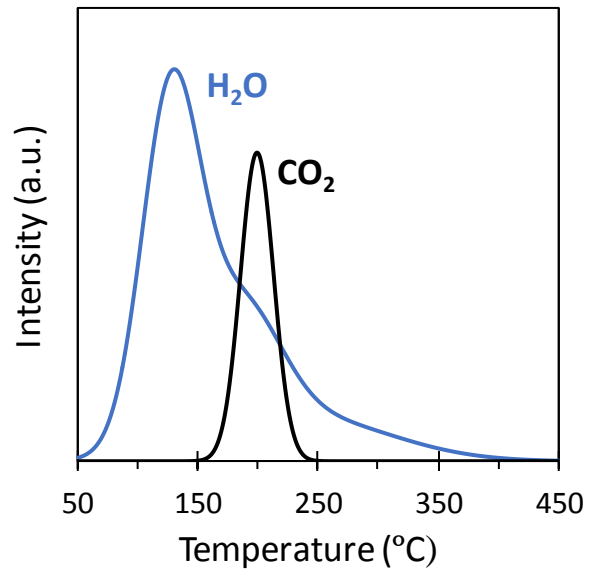


Figure 9

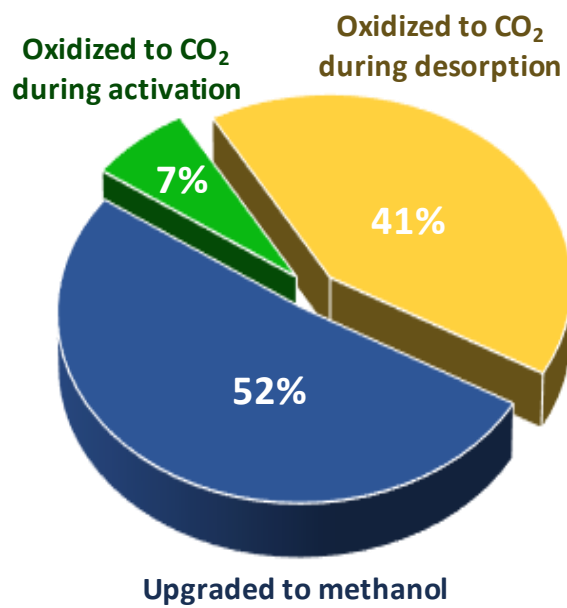


Table 1. Composition and morphological analysis (BET) of fresh and used Cu-exchanged mordenite

	Cu loading (wt. %)	Cu /Al (mol/mol)	BET surface area (m <sup>2</sup> /g)	Micropore volume (cm <sup>3</sup> /g)
Na – MOR	0	0	376	0.17
Cu – Na – MOR	4.5	0.54	359	0.15
Cu – Na – MOR (after 19 cycles)	4.5	0.54	350	0.14

Table 2. Summary of the optimal conditions for a reaction cycle. (Total gas flow and WHSV at desorption step consider the totality of the gas flow, composed by the N<sub>2</sub> flow and the water introduced)

	Adsorption	Desorption	Regeneration
Gas (mol%)	100 CH <sub>4</sub>	5.2 H <sub>2</sub> O + 96.8 N <sub>2</sub>	20 O <sub>2</sub> + 80 N <sub>2</sub>
Total Flow (mL n.t.p./min)	120	159	120
WHSV (Nm <sup>3</sup> h <sup>-1</sup> kg <sub>cat</sub> <sup>-1</sup> )	2.29	3.04	2.29
Temperature (°C)	200	150	450 (1°C/min)
Duration (min)	20	240	240